Supporting information

Controlling the Phase Segregation in Mixed Halide Perovskite through Nanocrystal Size

Andrés. F. Gualdrón-Reyes[#],[1,2,3] Seog Joon Yoon[#],[1] Eva M. Barea,[1] Said Agouram,[4] Vicente Muñoz-Sanjosé,[4] Ángel M. Meléndez[3] Martha E. Niño-Gómez[2,3], and Iván Mora-Seró [1*]

[1] Institute of Advanced Materials (INAM), University Jaume I, Avenida de Vicent Sos Baynat, s/n, 12006 Castelló de la Plana, Castellón, Spain

[2] Centro de Investigaciones en Catálisis (CICAT), Universidad Industrial de Santander, Sede UIS Guatiguará, Piedecuesta, Santander, Colombia. C.P. 681011.

[3] Centro de Investigación Científica y Tecnológica en Materiales y Nanociencias (CMN), Universidad Industrial de Santander, Piedecuesta, Santander, Colombia. C.P. 681011.

[4] Department of Applied Physics and Electromagnetism, University of Valencia, 46100 Valencia, Spain

*Corresponding author: sero@uji.es

#: equal contribution

Experimental section

Synthesis of colloidal $CsPbBr_{3-x}I_x$ nanoparticles

The synthesis of $CsPbBr_{3-x}I_x$ nanoparticle was performed according with the hot-injection method reported by Kovalenko and coworkers, with some modifications.[1, 2] All the chemicals used for carrying out this work were employed as received without any purification process. Briefly, a mixture composed by of 0.814 g of Cs_2CO_3, (202126, 99.9 %, Sigma-Aldrich) 2.5 mL of oleic acid (OA, 364525, 90 %, Sigma-Aldrich) and 40 mL of 1-octadecene (O806, 90 %, Sigma-Aldrich) was degasified in a 50 mL three neck-flask under vacuum for 90 min, and then heated at 140°C under N_2 conditions until Cs_2CO_3 reacted completely with OA. A translucid clear Cs-oleate solution was achieved. Before injection, the solution was preheated at 110°C keeping the N_2-purging, to avoid the precipitation of Cs-oleate. *Note* that *the appearance of a dark orange color in the Cs-oleate solution is indicative of Cs-oleate oxidation to form* Cs_2O.

To synthetize $CsPbBr_{3-x}I_x$ nanoparticles, 1.88 mmol of PbX_2 (PbI_2, 0.87 g, AB111058, 99.999 %, ABCR; $PbBr_2$, L0288, 0.69 g, 99.99 %, TCI) or their different halide compositions were added to 50 mL of ODE in a 100 mL three neck-flask. The mixture was dried under vacuum at 120°C for 90 min. Then, preheated OA and oleic acid (OLA, HT-OA100, 98 %, Sigma-Aldrich) (5 mL of each one) were loaded to the halide solution under N_2 conditions, and briefly it was degasified until the complete dissolution of halide precursors. Under N_2-purging, the temperature of reaction was raised to 170 °C and 190 °C, and 4 mL of Cs-oleate solution was quickly injected. Lastly, the reaction was quenched after adding the reaction flask in an ice bath for 5 and 20 s.

Isolation of $CsPbBr_{3-x}I_x$ nanoparticles

$CsPbBr_{3-x}I_x$ nanoparticle (x = 0.75) underwent two-purification process. For the first purification, 70 mL of anhydrous methyl acetate (MeOAc, 296996, 99.5%, Sigma-Aldrich) were added to 32 mL of as-synthesized nanoparticle dispersed solution and centrifuged at 7000 rpm for 10 min. The supernatant was discarded and the nanoparticle pellet was dispersed in 8 mL of hexane (CHROMASOLV, 34859, 99.7 %, Honeywell). For the second purification, 10 mL of anhydrous ethyl acetate (270989, 99.8 %, Sigma Aldrich) was added to the nanoparticle dispersion and then was rapidly centrifuged at 7000 rpm for 5 min. The nanoparticle pellet was dispersed in 10 mL of hexane and stored at low temperature for 48 h to precipitate Cs-oleate and Pb-oleate. The purified nanoparticle solution was decanted and dried under N_2 flow. Lastly, the $CsPbBr_{3-x}I_x$ nanoparticles (x = 0.75) were concentrated to 50 mg mL^{-1} with anhydrous octane (296988, 99 %, Sigma-Aldrich).

Fabrication of light-emitting diodes

FTO substrates (Pilkington, TEC-15) were rinsed with soap solution, Mili-Q water, acetone (211007.0716, 99.5 %, Panreac) and ethanol (141085.0716, 96 %, Panreac), each one for 15 min. After that, the substrates were dried with a compressed air and cleaned under UV-O_3 for 15 min. A TiO_2 compact layer was prepared by spin-casting 80 µL of a Ti-alkoxide solution (ShareChem, SC-BT060) at 4000 rpm for 30 s. Then, the as-prepared films were dried at 150 °C for 10 min and annealed at 500 °C for 30 min. $CsPbBr_{3-x}I_x$ nanoparticle layers were deposited by spin-coating the purified solution at 1000 rpm for 30 s. Then, each film was briefly added into a 10 $mgmL^{-1}$ $Pb(NO_3)_2$ (467790, 99.99 %, Sigma-Aldrich) in MeOAc, rinsed with neat MeOAc and dried with compressed air. The $Pb(NO_3)_2$/MeOAc solution was prepared following the procedure reported elsewhere.[3] The nanoparticle deposition and dipping into $Pb(NO_3)_2$/MeOAc solution was repeated 4 times. The spiro-OMeTAD (792071, 99 %, Sigma-Aldrich) hole transporting material was deposited on nanoparticle films by spin-coating at 4000 rpm for 30 s from a solution of 72.3 mg of spiro-OMeTAD, 1 ml anhydrous chlorobenzene (284513, 99.8 %, Sigma-Aldrich), 28.8 µL of 4-TB (142379, 96 %, Sigma-Aldrich), and 17.5 µL of Li-TFSI solution (520 mg/ml in acetonitrile, 271004, 99.8 %, Sigma-Aldrich). Finally, Au electrode was thermally evaporated at a rate from 0.5-1 A/s. For LEDs measurements, the active areas were encapsulated with adhesive tape and then with a UV photo-curable epoxy resin from Lighting Enterprises (ELC4908-30) cover glass. For studying the morphology, crystallinity and photophysical properties of $CsPbBr_{3-x}I_x$ nanoparticle and bulk films, inside N_2 filled glove box, as-prepared colloidal solutions were drop-casted in glove box on glasses (25 x 25 mm) previously rinsed and cleaned. Ligand exchange were proceeded through dipping films into 10 mg mL^{-1} $Pb(NO_3)_2$ in MeOAc. Consequently, the films were rinsed with neat MeOAc and then they were dried with compressed air. Perovskite nanoparticle films were annealed at 225 °C, varying the annealing time for 5, 10, 20, 30, 60 and 180 s, to obtain bulk films. To protect the perovskite nanoparticles and annealed films from the ambient air, 10 $mgmL^{-1}$ of poly-methyl methacrylate (PMMA, 182230, M_n 120000, Sigma-Aldrich) in anhydrous chlorobenzene was also drop-casted after film deposition.

Characterizations

The steady state absorption spectra of colloidal $CsPbBr_{3-x}I_x$ perovskite nanoparticle solutions and films were achieved by using a UV/Vis absorption spectrophotometer (Varian, Cary 300), with and without 0.1 sun illumination (10 $mWcm^{-2}$) by using a Class A solar simulator (from Abet Technologies Sun 2000) with neutral density filter. The emission measurements were collected by a Horiba Fluorolog 3-11. The change of the emission features of the QDs and bulk films over the time

was monitored with an Andor monochromator system with a DV420A-OE charged coupled device (CCD) camera as detector. 405 and 532 nm continuous-wave (CW) 180 mW laser was on a home-built optic system. The CW lasers irradiated the perovskite films with 10 mW cm^{-2} (405 nm CW laser). Note that it has been reported a threshold for observing phase-segregation (0.04 mW/cm^2) at irradiation power four orders of magnitude lower than the used in this work.[4] 435 nm long pass filters were applied to cut off additional light from laser. Various neutral density were applied in front of the detector to control emission intensities. X-ray diffraction (XRD) patterns of the nanoparticle and bulk films were achieved with a D4 Endeavor diffractometer from Bruker-AXS, using a Cu Kα radiation source (λ = 1.54056 Å). High-resolution transmission electron microscopy (HRTEM) images of perovskite nanoparticles were obtained with a field emission gun TECNAI G2 F20 microscope operated at 200 kV. For the perovskite films, field emission scanning electron microscopy (FESEM) images were achieved by using a JSM7001F microscope. The roughness and surface potential were studied with an atomic force microscopy with Kelvin prove (Concept Scientific Instrument). The absolute photoluminescence quantum yield (PLQY) of the colloidal nanoparticle solutions was estimated with a Hamamatsu PLQY Absolute QY Measurement System C9920-02, equipped with an integrating sphere, at an excitation wavelength of 400 nm. The electroluminescence properties of the $CsPbBr_{3-x}I_x$ film-based devices were measured in a DV420A-OE CCD camera, by applying a bias voltage of 9 V for 120 s with a Gamry 600 potentiostat. The generated current was registered by achieving chronoamperometric profile.

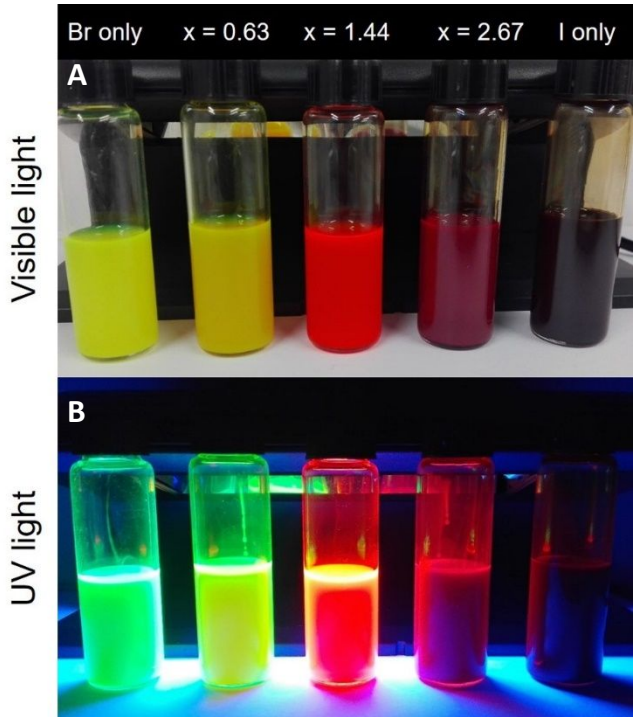

Figure S1. Colloidal $CsPbBr_{3-x}I_x$ nanoparticle solutions varying the halide composition (x = Br/(Br+I)) under visible (A) and UV illumination (B).

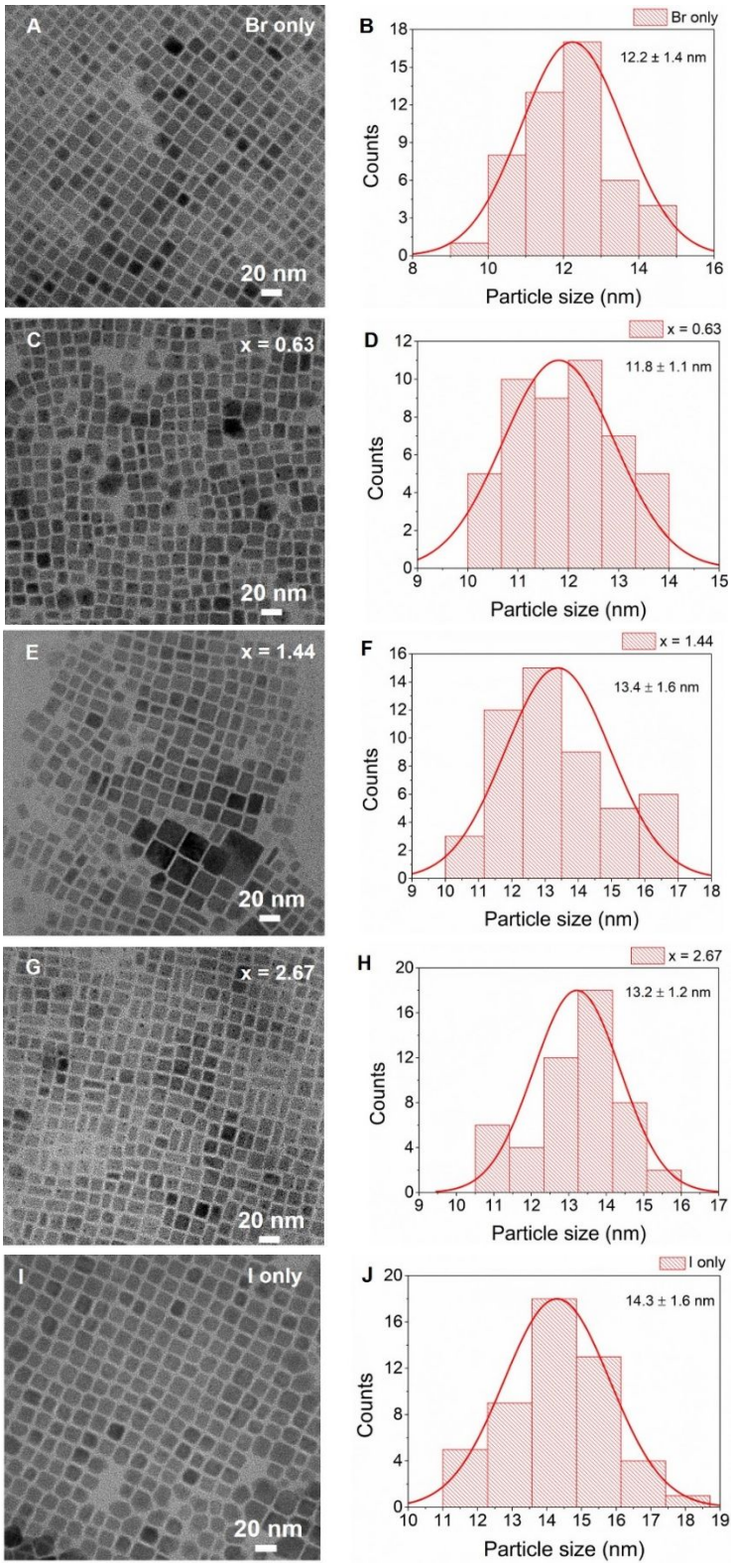

Figure S2. TEM images of the colloidal $CsPbBr_{3-x}I_x$ nanoparticles obtained by varying the halide composition: (A,B) x = 0, (C,D) x = 0.63, (E,F) x = 1.44, (G,H) x = 2.67 and (I,J) x = 3.

Table S1. Chemical composition of $CsPbBr_{3-x}I_x$ nanoparticles including de nominal composition from the rate of precursor utilized in the synthesis and calculated in the synthesized nanoparticles by two methods: i) EDX from TEM characterization and ii) through (200) peak in XRD patterns in Figure S8A by following literature[5].

Nominal Br : I ratio (in precursor)	Br/(I+Br) Nominal	I (at. %) EDX	Cs (at.%) EDX	Pb (at. %) EDX	Br (at.%) EDX	Br/(I+Br) EDX	Br/(I+Br) Calculated w/ XRD (200)*
Br only	1	0	28.2 ± 2.5	24.5 ± 2.5	47.3 ± 1.5	1	
x = 0.63	0.79	11.1 ± 2.0	26.0 ± 2.2	22.3 ± 2.6	40.6 ± 2.0	0.79	0.87
x = 1.44	0.52	24 ± 5	27 ± 3	22.4 ± 2.9	27 ± 3	0.52	0.54
x = 2.67	0.11	51 ± 3	24.3 ± 2.5	18.9 ± 2.0	6.0 ± 2.0	0.11	0.07
I only	0	63 ± 4	20.7 ± 2.0	16.2 ± 2.0	0	0	

* Based on (200) peaks in Figure S8A.

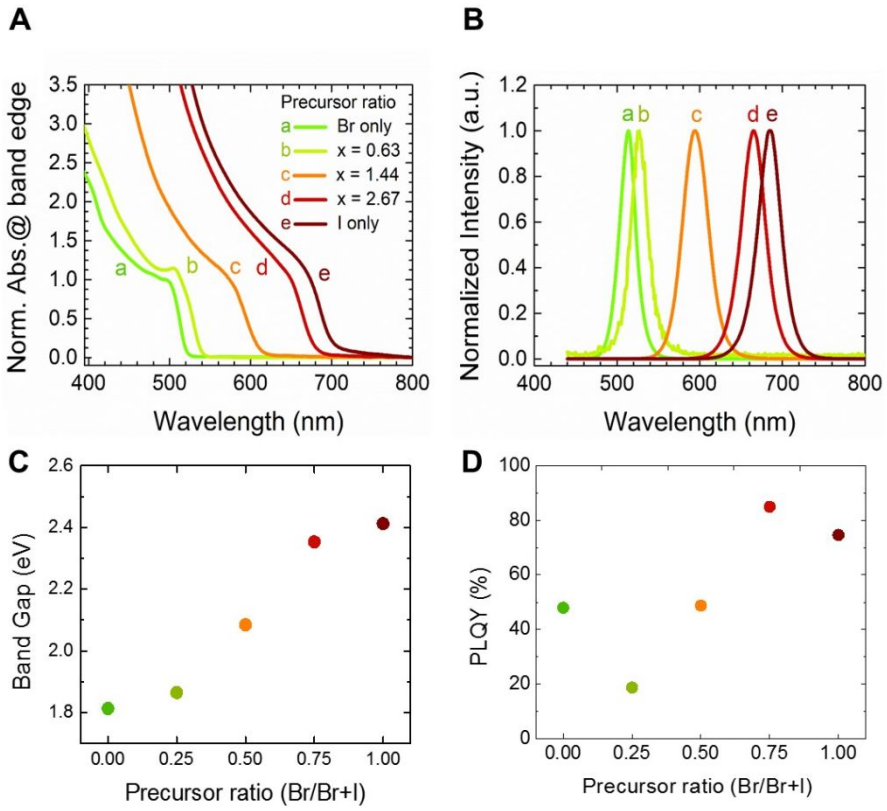

Figure S3. Photophysical properties of $CsPbBr_{3-x}I_x$ nanoparticles dispersed in hexane: (A) absorption, (B) emission, (C) estimated band gap and (D) photoluminescence quantum yield (PLQY), as a function of the halide composition.

Table S2. Optical parameters of the colloidal $CsPbBr_{3-x}I_x$ nanoparticles.

Precursor ratio (Br/Br+I)	Band edge through Abs. (nm)	Emission peak position (nm)	Band gap (eV)	PL QY (%)
Br only	495	514	2.41	48.0
x = 0.63	504	527	2.35	18.8
x = 1.44	574	595	2.08	48.8
x = 2.67	650	665	1.86	84.9
I only	674	684	1.81	74.6

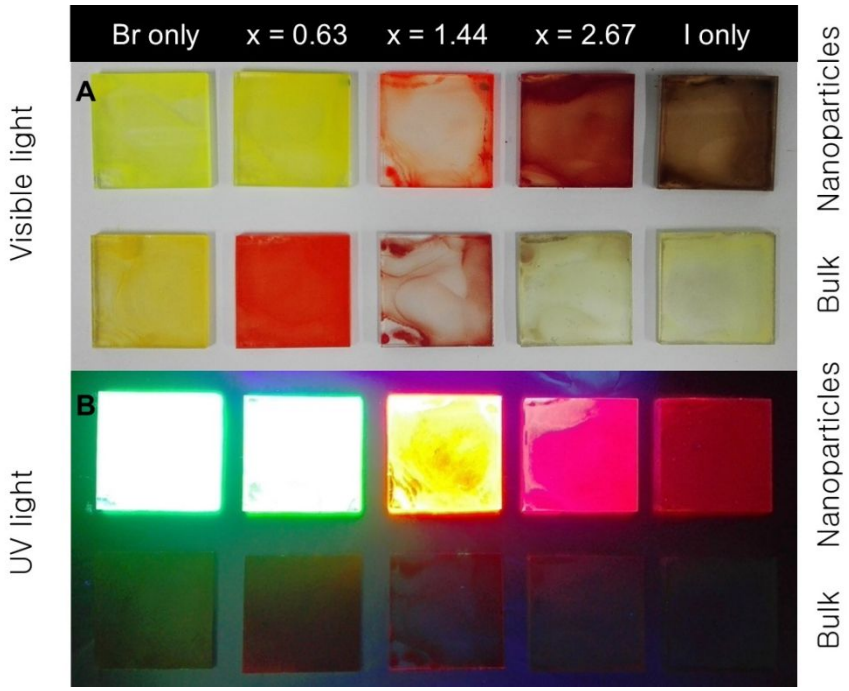

Figure S4. $CsPbBr_{3-x}I_x$ nanoparticle deposited film and bulk films obtained after annealing at 225°C for 180 s, varying the halide composition under (A) visible and (B) UV illumination.

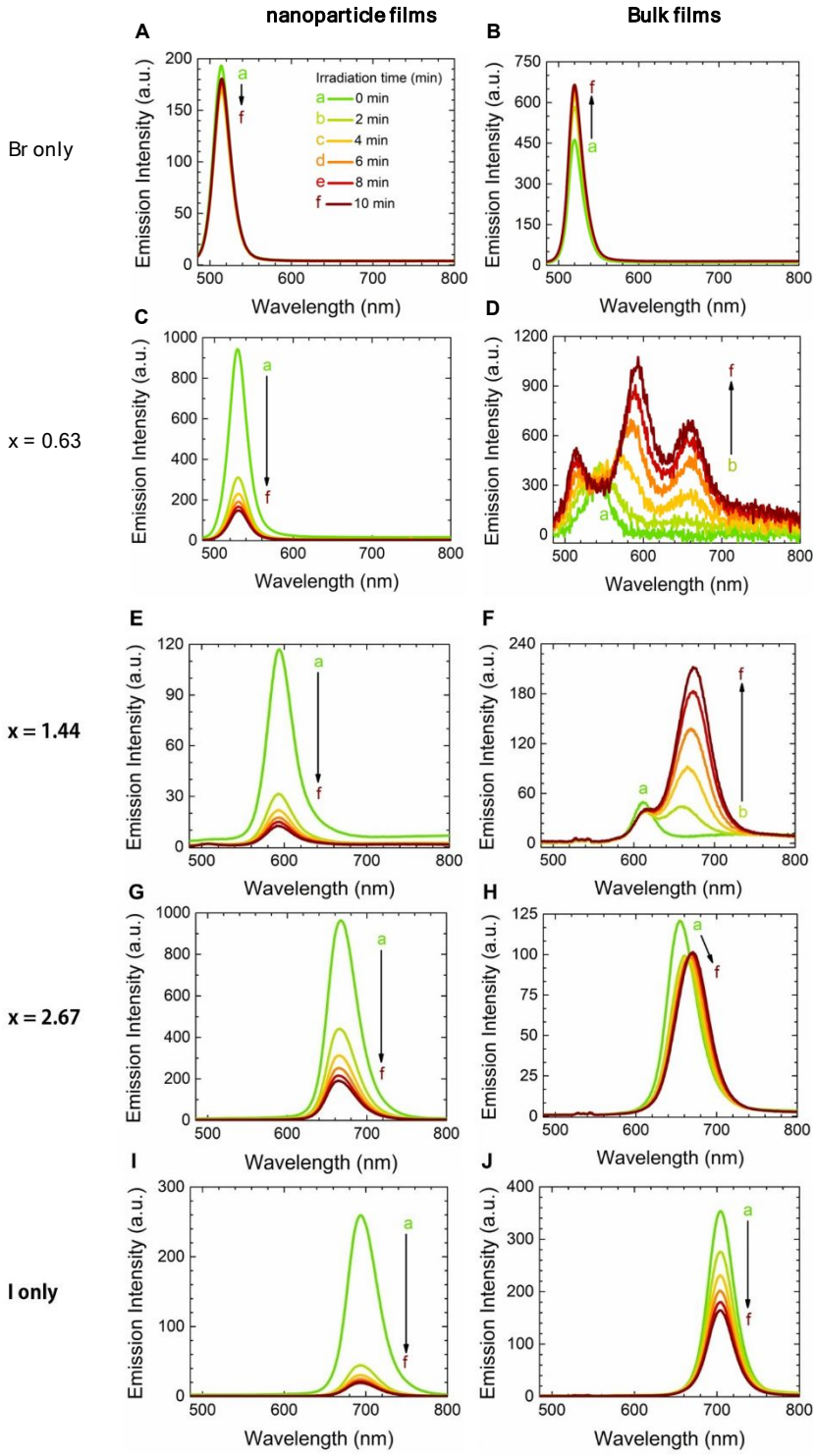

Figure S5. Emission spectra monitored under 10 min of CW excitation (I_{exc} = 10 mW cm^{-2}) for the $CsPbBr_{3-x}I_x$ nanoparticle (A,C,E,G,I) and bulk films (B,D,F,H,J) obtained after annealing at 225°C for 180 s.

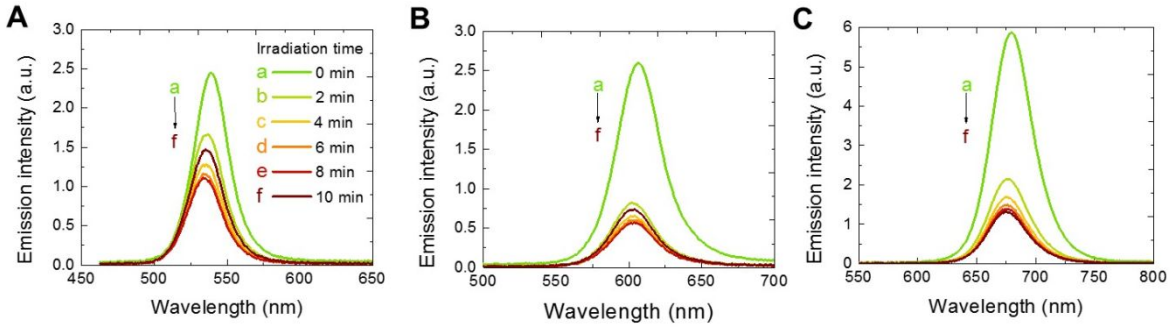

Figure S6. Emission spectra monitored under 10 min of CW excitation (I_{exc} = 10 mWcm^{-2}) for the $CsPbBr_{3-x}I_x$ nanoparticles in PMMA matrix for (A) x = 0.63, (B) x = 1.44 and (C) x = 2.67.

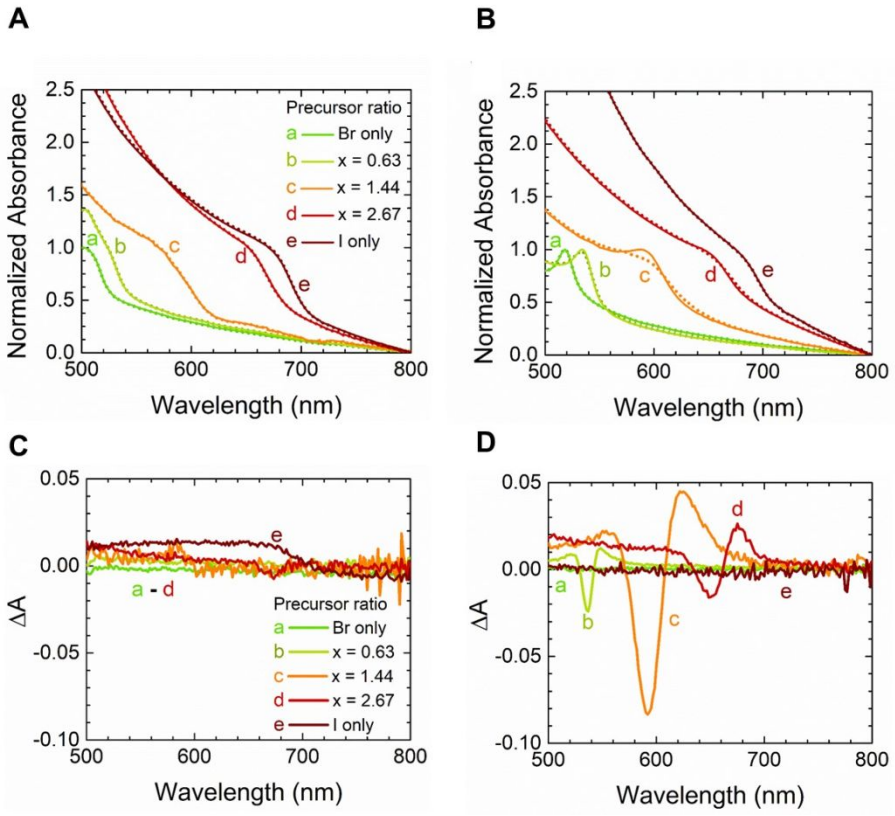

Figure S7. (A,B) Absorption spectra (A: nanoparticle film, B: bulk film) both just after photoirradiation (0.1 sun, dot line) and 45 min after irradiation in dark condition (straight line). (C,D) Absorption changes (ΔA) after storing in dark, (C) for nanoparticle film (D) and bulk films. Bulk films obtained after annealing at 225°C for180 s.

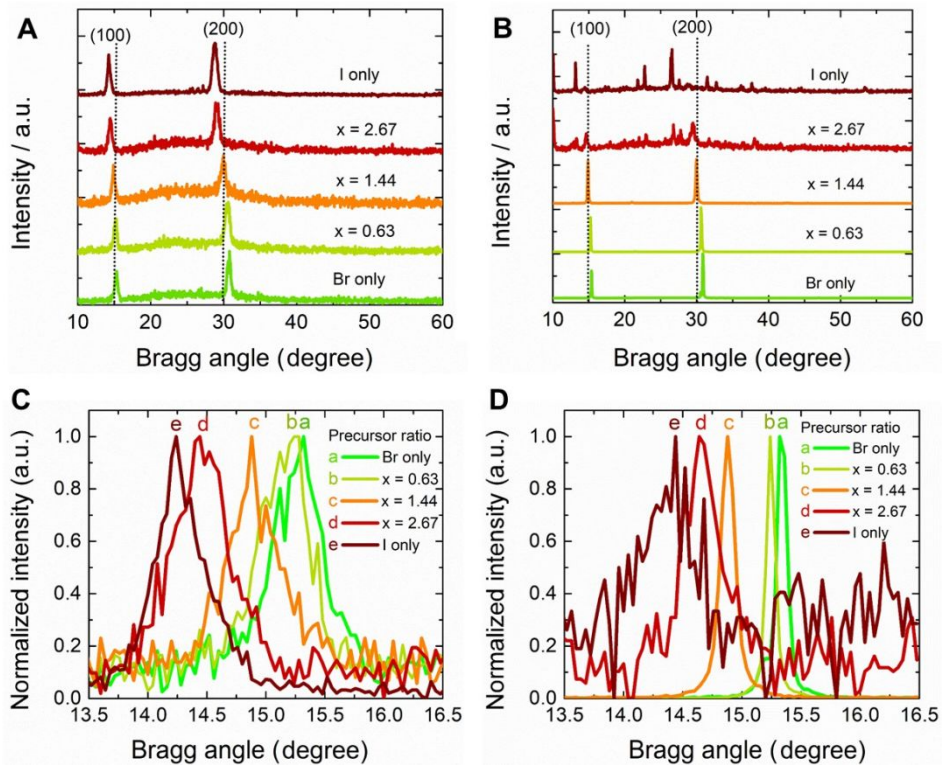

Figure S8. XRD patterns of the $CsPbBr_{3-x}I_x$ (A) nanoparticle films and (B) bulk films after annealing at 225°C for 180 s. (C) and (D) Enlarged of the (100) peak for the perovskites described respectively in (A) and (B).

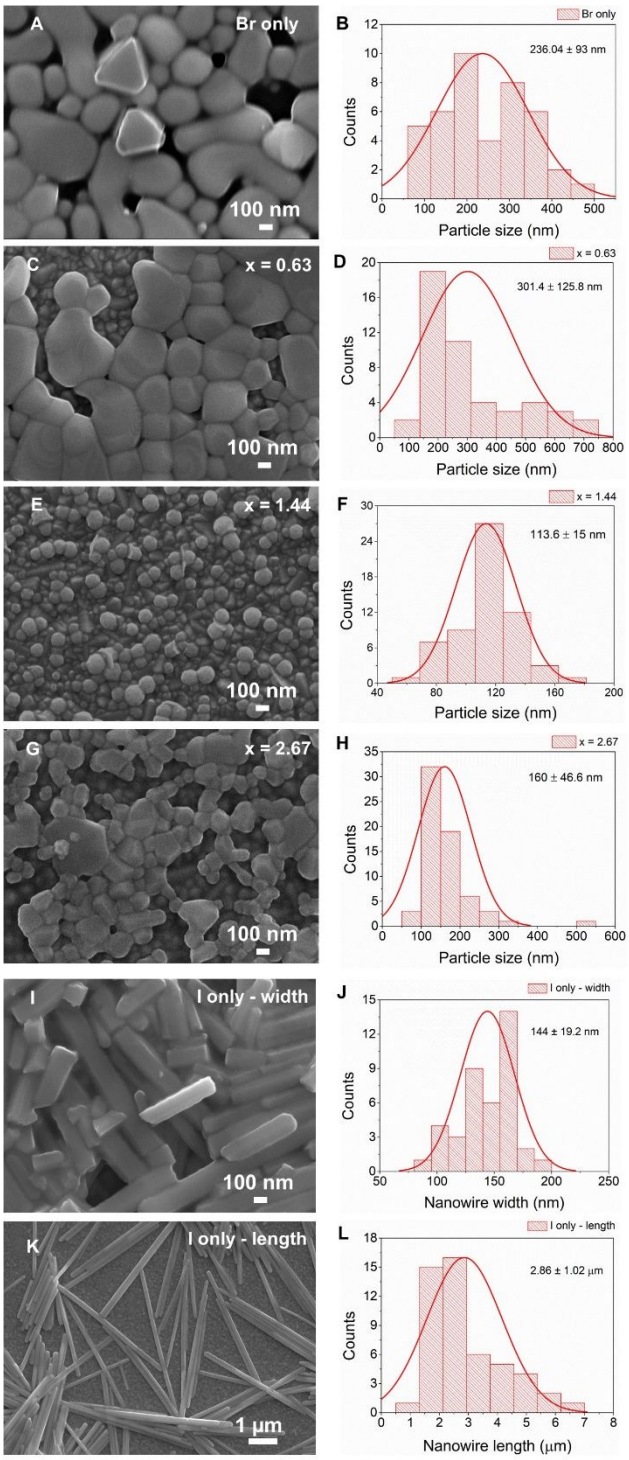

Figure S9. SEM images of the $CsPbBr_{3-x}I_x$ bulk films (A, C, E, G, I, K) after annealing at 225°C for 180 s, varying the halide composition. Histograms (B, D, F, H, J, L) were achieved to determine the average grain sizes from perovskite micrographs.

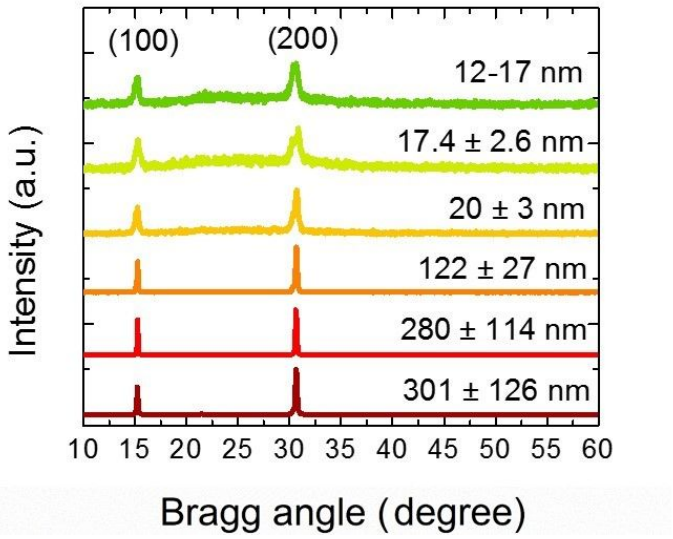

Figure S10. XRD patterns of the $CsPbBr_{3-x}I_x$ bulk films with various crystalline sizes determined by SEM obtained at 225°C during different annealing time.

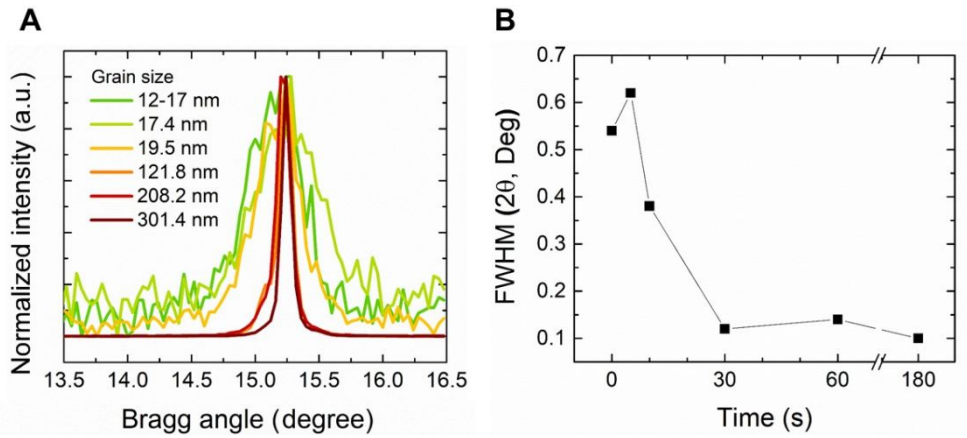

Figure S11. (A) Enlarged (100) peak in XRD patterns from $CsPbBr_{3-x}I_x$ films (x = 0.63) in Figure S10 with different grain size. The bigger crystalline sizes were obtained by increasing annealing time. (B) Full width at half maximum (FWHM) obtained from (100) peak as a function of annealing time.

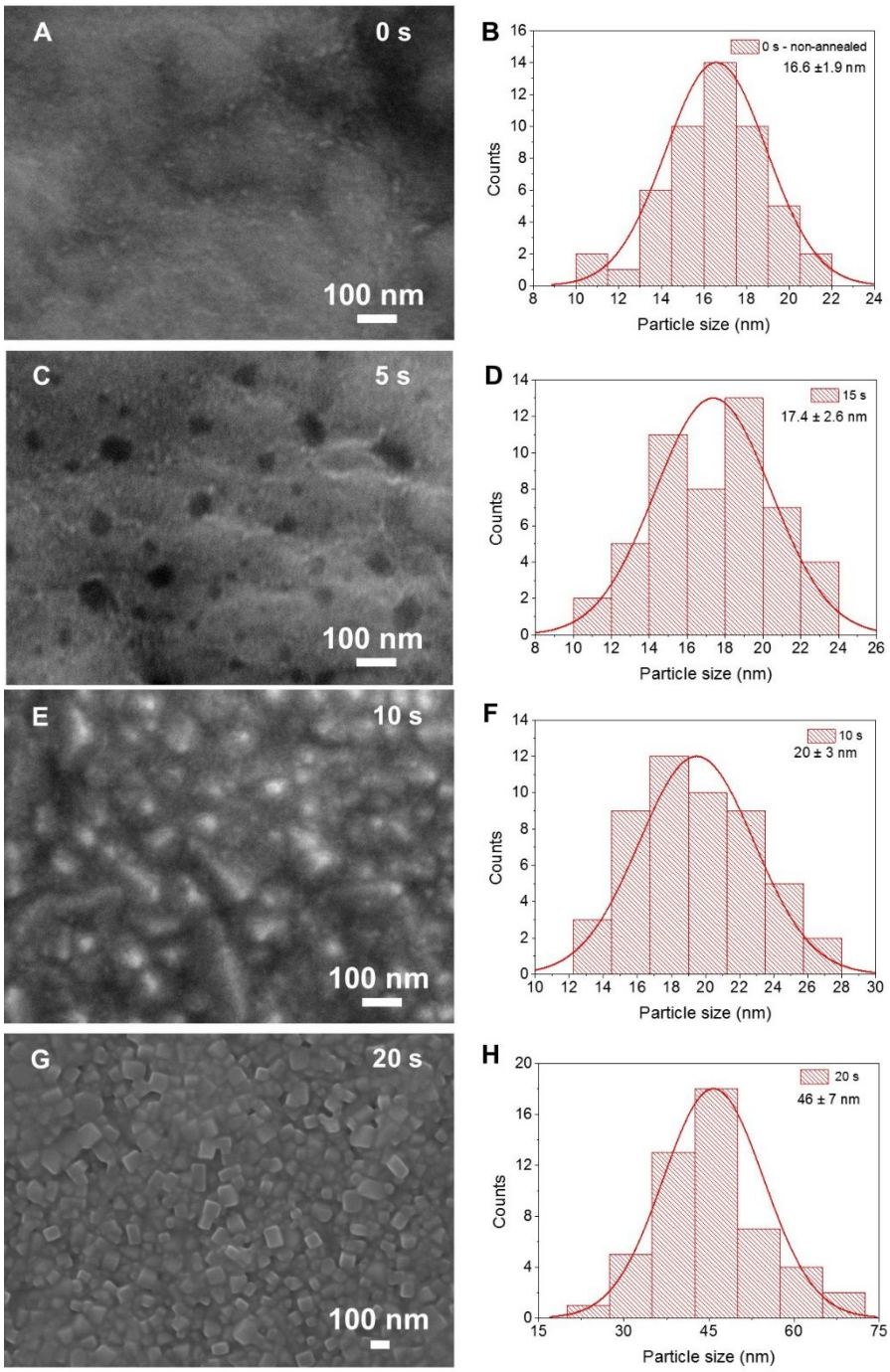
A
0 s
100 nm
B
0 s - non-annealed
16.6 ±1.9 nm
Counts
Particle size (nm)
C
5 s
100 nm
D
15 s
17.4 ± 2.6 nm
Counts
Particle size (nm)
E
10 s
100 nm
F
10 s
20 ± 3 nm
Counts
Particle size (nm)
G
20 s
100 nm
H
20 s
46 ± 7 nm
Counts
Particle size (nm)

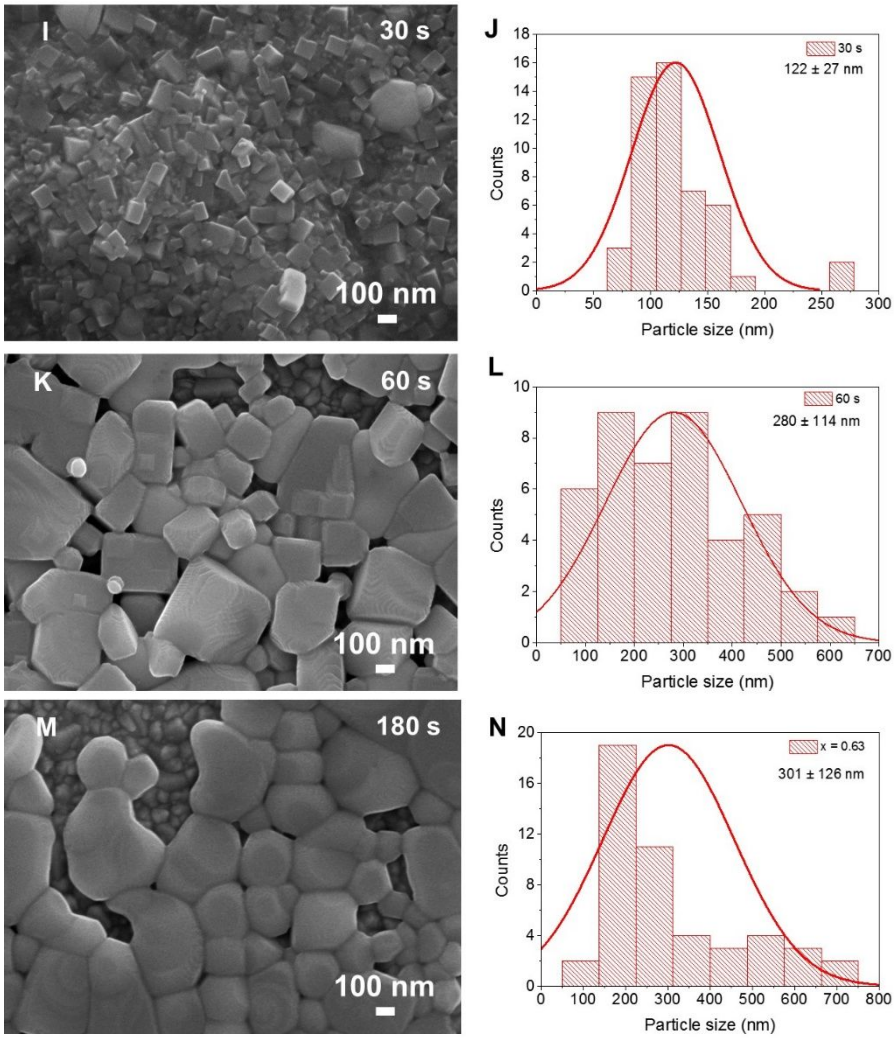

Figure S12. SEM images of the $CsPbBr_{3-x}I_x$ bulk films (x = 0.63) obtained at 225°C, varying the annealing time (A, C, E, G, I, K, M). Histograms (B, D, F, H, J, L, N) were achieved to determine the average grain sizes from perovskite micrographs. The $CsPbBr_{3-x}I_x$ were deposited on FTO to reduce charging effect while SEM measurement.

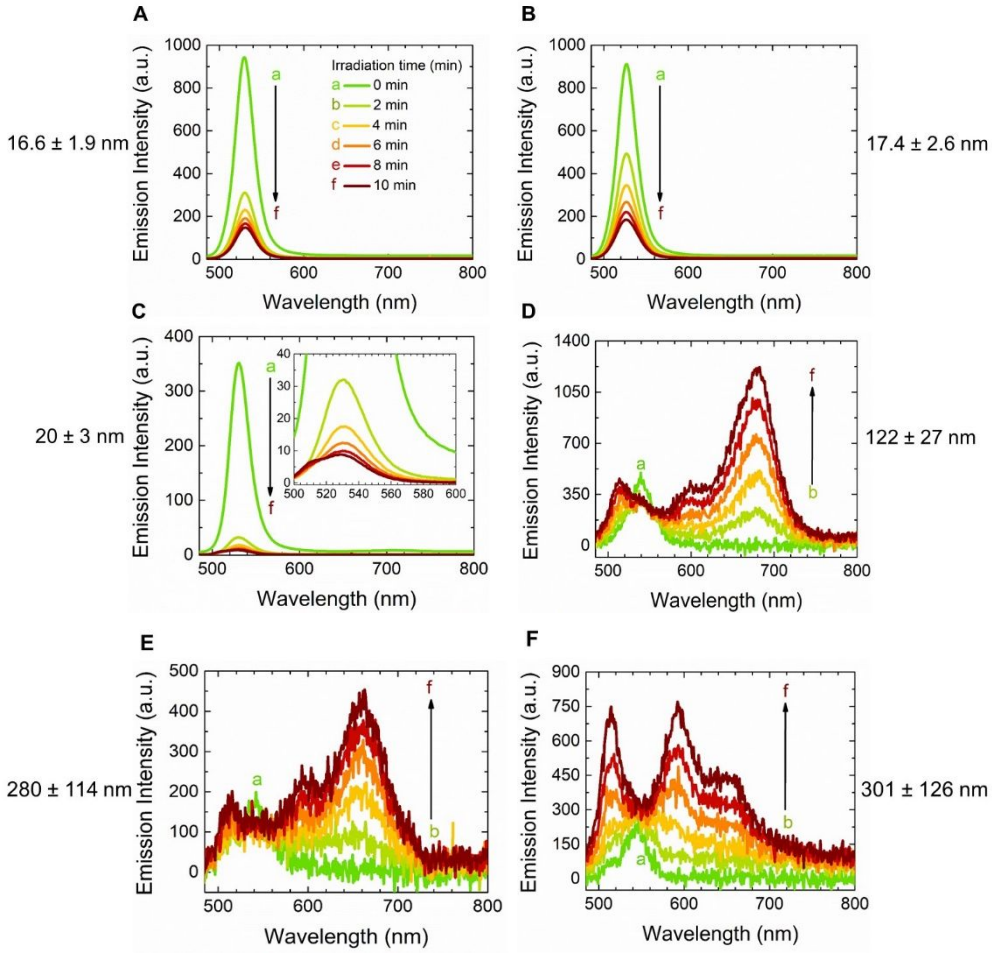

Figure S13. Emission spectra monitored under 10 min of CW excitation (I_{exc} = 10 mWcm^{-2}) for the $CsPbBr_{3-x}I_x$ bulk films (x = 0.63) with different crystalline sizes as follows: (A) 16.6 nm, (B) 17.4 nm, (C) 19.5 nm, (D) 121.9 nm, (E) 280.2 nm, and (F) 301.4 nm.

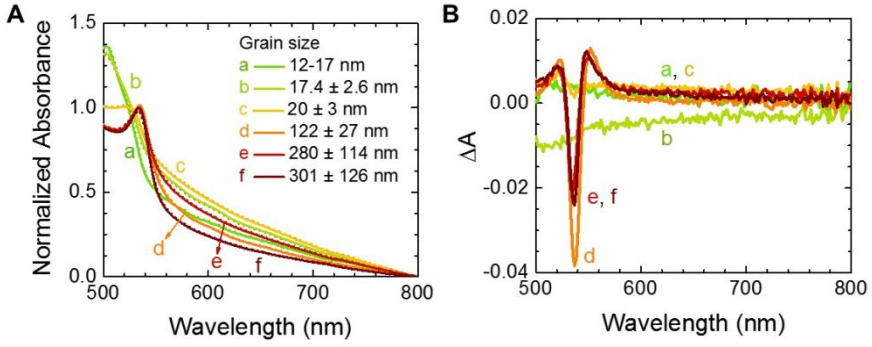

Figure S14. (A) Absorption spectra and (B) their corresponding absorption changes (ΔA) for $CsPbBr_{3-x}I_x$ (x = 0.63) bulk films obtained after annealing at 225°C by varying the crystalline sizes (a-f) before (solid line) and after (dash line) 10 min under 0.1 sun illumination (I_{exc} = 10 mWcm^{-2}).

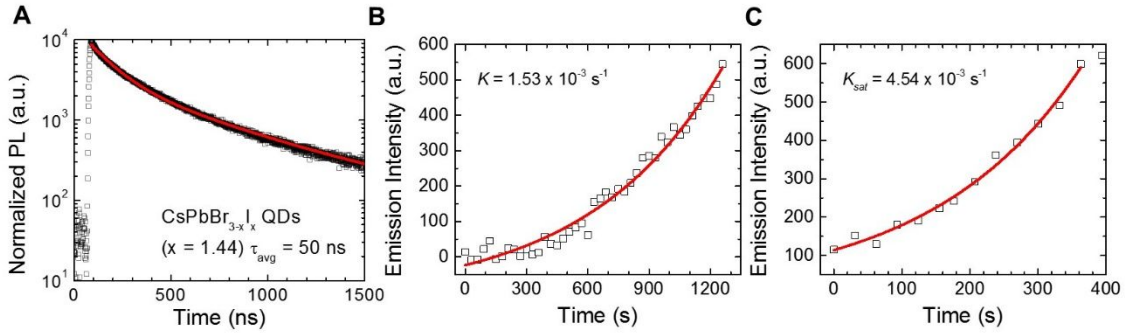

Figure S15. (A) Time-resolved photoluminescence decay for the colloidal $CsPbBr_{3-x}I_x$ nanoparticle solution (x = 1.44). Bi-exponential fittings ($y = y_0 + A_1 e^{-x/\tau_1} + A_1 e^{-x/\tau_2}$) and calculation of average lifetime ($\tau_{avg} = \frac{\Sigma A_i \tau_i^2}{\Sigma A_i \tau_i}$) were done by following literature.[6, 7] (B,C) pseudo-first order kinetic analysis by monitoring emission evolution from the segregated I-rich domain (at 658 nm) for $CsPbBr_{3-x}I_x$ bulk films with different grain sizes: (B) 45.8 nm and (C) 301 nm. Exponential growth fitting ($y = y_0 + A_1 e^{(x - x_0)/\tau_1}$) were performed to calculate the segregation rate (K) for 45.8 nm (B) and saturated segregation rate (K_{sat}) for 301 nm grain size (C).

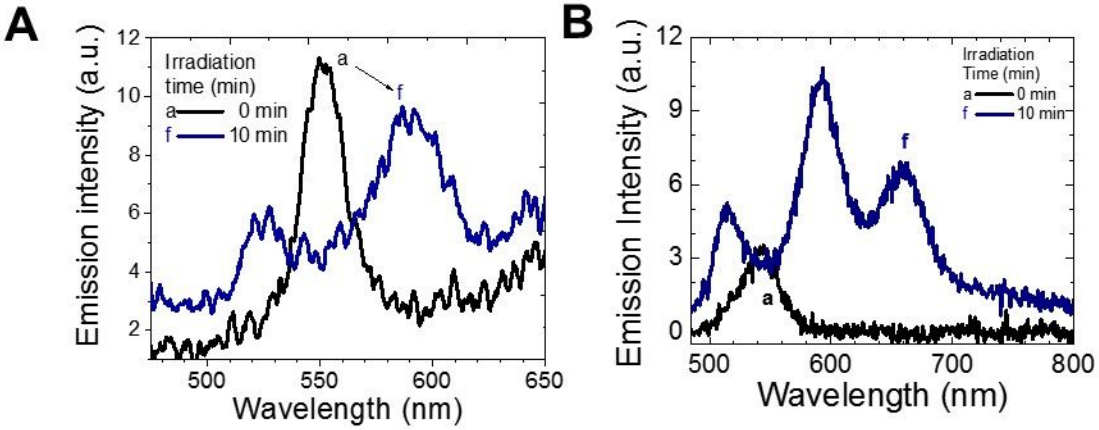

Figure S16. Emission spectra monitored under 10 min of CW excitation (I_{exc} = 10 $mWcm^{-2}$) for the $CsPbBr_{3-x}I_x$ bulk films (x = 0.63, grain size: 301 ± 126 nm) (A) without ligand exchange process before annealing process to form bulk film and (b) with ligand exchange process.

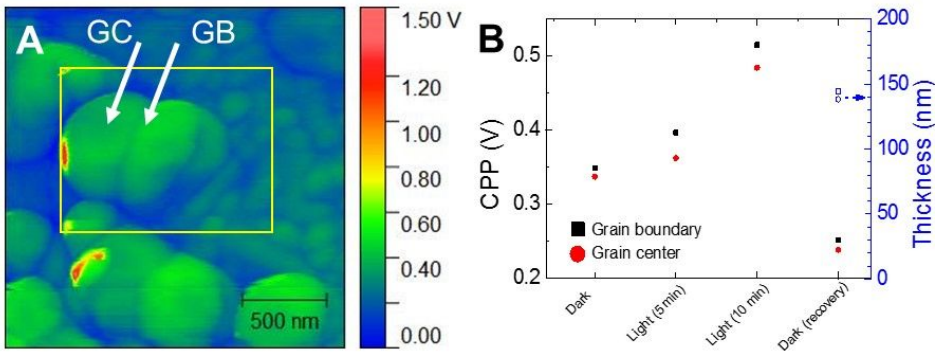

Figure S17. (A) KPFM image obtained for the $CsPbBr_{3-x}I_x$ bulk film (x = 0.63) with 121.8 nm grain size, after 5 min of photoirradiation. (B) CPP at grain boundary (square) and at grain center (circle) with subsequent dark, photoirradiation, and dark condition. The positions of grain boundary and grain center were marked (A) Potential difference (ΔV) in the grain center (GC) and grain boundary (GB) were measured during the dark, illumination and recovery processes.

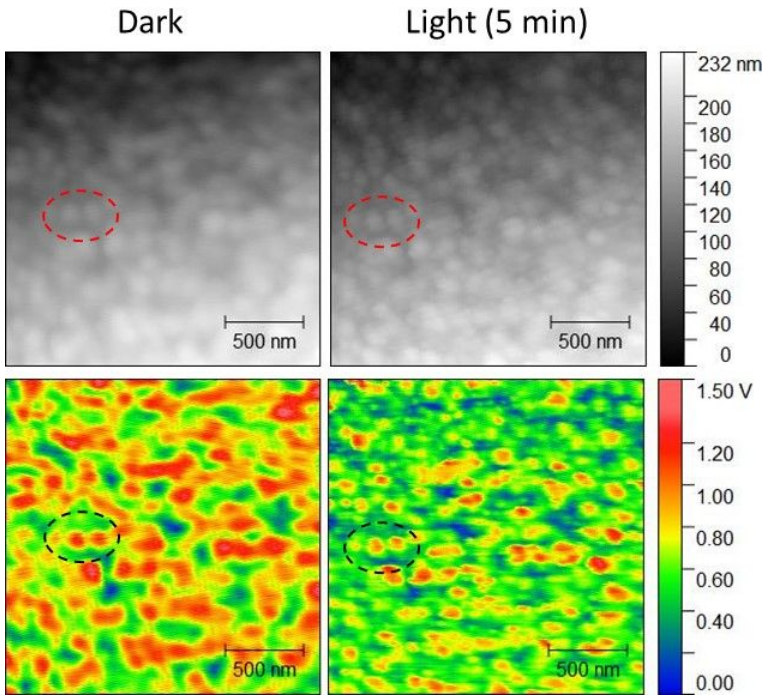

Figure S18. KPFM image obtained for the $CsPbBr_3$ bulk film with 121.8 nm grain size, before (dark) and after 5 min of photoirradiation (Light 5 min). Circled area was used to measure difference of CPP value following Figure S19.

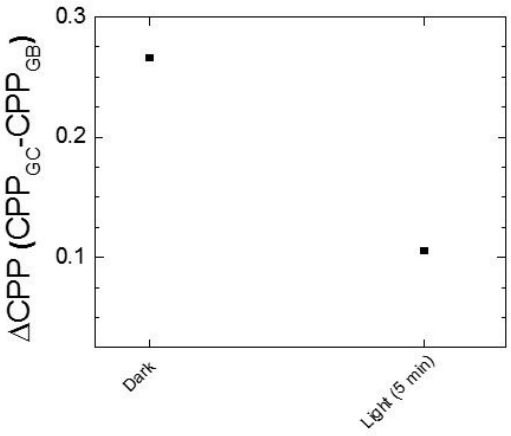

Figure S19. Potential difference (ΔV) in the grain center (GC) and grain boundary (GB) as marked in Figure S18 with and without photoirradiation.

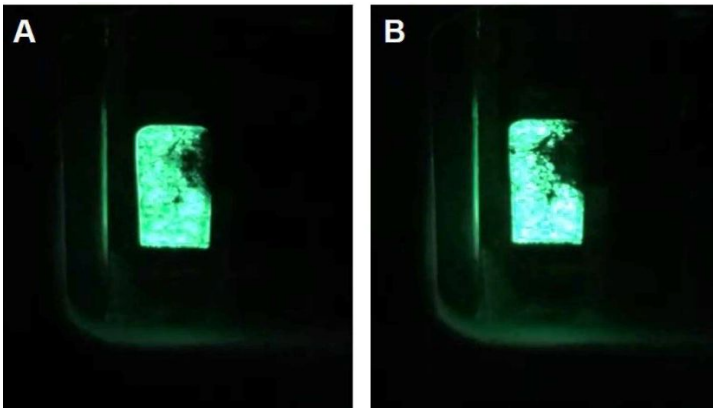

Figure S20. Green-light emission while electroluminescence measurement for $CsPbBr_{3-x}I_x$ nanoparticle film (x = 0.63) based LED device under 9 V (A) before and (B) after 120 s.

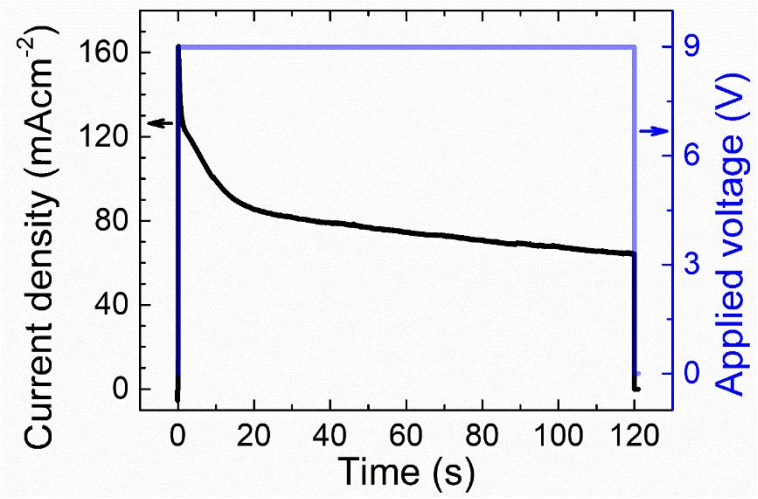

Figure S21. Chronoamperometric profile of devices achieved under 9 V for 120 s.

Supplementary Note 1. Calculation of diffusion length

The diffusion length (L) was calculated through empirically derived equation from literature.[4]

$$K = K_{sat}(1 - e^{-\beta I_{exc}}) \quad (1)$$

K, K_{sat}, β, and I_{exc}, represent segregation rate of the film with 45.8 nm grain size (Figure S15B, 1.53 x 10^{-3} s^{-1}), segregation rate of film with 301.8 nm grain size (Figure S15C, 4.54 x 10^{-3} s^{-1}), empirical fitting parameter, and power density of excitation source (405 nm CW laser with 10 $mWcm^{-2}$), respectively. K is the intermediate segregation rate in the 45.8 nm sized grain. K_{sat} is saturated segregation rate, which electron/hole can diffuse in large grain with its own diffusion length. We assume that segregation rate is dependent to particle size. While annealing and agglomeration stage, the electron/hole diffusion is confined in grains, which are less than 100 nm.[4]

Through the equation 1, we could calculate:

$$\beta = 4.12 \times 10^{-2}\ cm^2\ mW^{-1} \quad (2)$$

The empirical fitting parameter β can be used as follows:

$$\beta = \frac{V_D \rho}{I_{exc}} = \frac{V_D \alpha \tau}{h\nu_{exc}} \quad (3)$$

$$V_D = \frac{4}{3}\pi L^3 \quad (4)$$

V_D, ρ, α, τ, and $h\nu_{exc}$ represent diffusion volume, photogenerated carrier density, absorption cross section (10^5 cm^{-1}), emission lifetime of the mixed halide perovskite QD (50 ns, as shown in Figure

14A), and 3.06 eV photon^{-1} = 4.90 x 10^{-19} W·s, respectively. By putting the parameters to equation 3.4, *L* can be derived as 45.8 nm.

References

(1) Protesescu, L.; Yakunin, S.; Bodnarchuk, M. I.; Krieg, F.; Caputo, R.; Hendon, C. H.; Yang, R. X.; Walsh, A.; Kovalenko, M. V. Nanocrystals of Cesium Lead Halide Perovskites ($CsPbX_3$, X = Cl, Br, and I): Novel Optoelectronic Materials Showing Bright Emission with Wide Color Gamut. *Nano Lett.* **2015**, *15*, 3692-3696.

(2) Nedelcu, G.; Protesescu, L.; Yakunin, S.; Bodnarchuk, M. I.; Grotevent, M. J.; Kovalenko, M. V. Fast Anion-Exchange in Highly Luminescent Nanocrystals of Cesium Lead Halide Perovskites ($CsPbX_3$, X = Cl, Br, I). *Nano Lett.* **2015**, *15*, 5635-5640.

(3) Sanehira, E. M.; Marshall, A. R.; Christians, J. A.; Harvey, S. P.; Ciesielski, P. N.; Wheeler, L. M.; Schulz, P.; Lin, L. Y.; Beard, M. C.; Luther, J. M. Enhanced mobility $CsPbI_3$ quantum dot arrays for record-efficiency, high-voltage photovoltaic cells. *Sci. Adv.* **2017**, *3*, eaao4204.

(4) Draguta, S.; Sharia, O.; Yoon, S. J.; Brennan, M. C.; Morozov, Y. V.; Manser, J. S.; Kamat, P. V.; Schneider, W. F.; Kuno, M. Rationalizing the light-induced phase separation of mixed halide organic-inorganic perovskites. *Nat. Commun.* **2017**, *8*, 200.

(5) Brennan, M. C.; Draguta, S.; Kamat, P. V.; Kuno, M. Light-Induced Anion Phase Segregation in Mixed Halide Perovskites. *ACS Energy Lett.* **2018**, *3*, 204-213.

(6) Ravi, V. K.; Scheidt, R. A.; Nag, A.; Kuno, M.; Kamat, P. V. To Exchange or Not to Exchange. Suppressing Anion Exchange in Cesium Lead Halide Perovskites with $PbSO_4$–Oleate Capping. *ACS Energy Lett.* **2018**, *3*, 1049-1055.

(7) Hines, D. A.; Becker, M. A.; Kamat, P. V. Photoinduced Surface Oxidation and Its Effect on the Exciton Dynamics of CdSe Quantum Dots. *J. Phys. Chem. C* **2012**, *116*, 13452-13457.